Upstream Polybasic Region in Peptides Enhances Dual Specificity for Prenylation by Both Farnesyltransferase and Geranylgeranyltransferase Type I†

Katherine A. Hicks,‡ Heather L. Hartman,‖ and Carol A. Fierke*,‡,‖

Departments of Biological Chemistry and Chemistry, University of Michigan, Ann Arbor, Michigan 48109

Received May 23, 2005; Revised Manuscript Received September 13, 2005

ABSTRACT: Protein farnesyltransferase (FTase) and protein geranylgeranyltransferase type I (GGTase I) catalyze the attachment of a farnesyl or geranylgeranyl lipid, respectively, near the C-terminus of their protein substrates. FTase and GGTase I differ in both their substrate specificity and magnesium dependence, where the activity of FTase, but not GGTase I, is activated by magnesium. Many protein substrates of these enzymes contain an upstream polybasic region that is proposed to increase the affinity of the substrate and aid in plasma membrane association. Here, we demonstrate that the addition of an upstream polybasic region to a peptide substrate enhances the binding affinity of FTase ∼4-fold for the peptide but diminishes the catalytic efficiency of the reaction, reflected by decreases in both the prenylation rate constant and k_{cat}/K_M. Specifically, the prenylation rate constant decreases 7-fold at 5 mM $MgCl_2$ for the peptide KKKSKTKCVIM (C-terminal sequence of K-Ras4B) in comparison to TKCVIM. This decrease is accompanied by an alteration in the dependence on magnesium, as the K_{Mg} increases from 2.2 ± 0.1 mM for TKCVIM to 11.5 ± 0.1 mM for KKKSKTKCVIM. The presence of an upstream polybasic region does not significantly affect GGTase I-catalyzed reactions, as only minimal changes are seen in K_d, k_{cat}/K_M, and k_{chem} values. Thus, the presence of an upstream polybasic region enhances the dual prenylation of these substrates, by decreasing the catalytic efficiency of farnesylation catalyzed by FTase to a level comparable to that of geranylgeranylation catalyzed by GGTase I.

Protein farnesyltransferase (FTase)[1] and protein geranylgeranyltransferase type I (GGTase I) are members of a class of enzymes known as protein prenyltransferases that catalyze the attachment of hydrophobic isoprenoid groups, known as prenyl groups, onto the cysteine sulfur of protein substrates. Prenylation is required for membrane association and protein function (*1*). FTase attaches a 15-carbon prenyl group onto its protein substrates, which is donated from farnesyl diphosphate (FPP), while GGTase I catalyzes the transfer of a 20-carbon prenyl group from geranylgeranyl diphosphate (GGPP). FTase and GGTase I are heterodimeric enzymes with a common α-subunit and β-subunits that are 30% identical (*1*). FTase and GGTase I contain a catalytic zinc ion that coordinates the thiol of the peptide substrate. Magnesium ions activate FTase, but not GGTase I (*2*−*4*). The kinetic pathway for these enzymes has a preferred binding order with FPP or GGPP binding before the protein substrate, followed by a rapid prenylation step and slow product dissociation (Scheme 1) (*5*, *6*). In general, the prenylation rate constant (k_{chem}) catalyzed by GGTase is ∼20-fold slower than the farnesylation rate constant catalyzed by FTase (*2*).

Scheme 1: Minimal FTase Kinetic Mechanism[a]

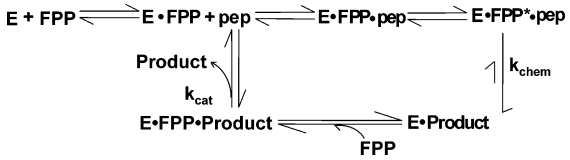

[a] In the GGTase I-catalyzed reaction, the prenyl group is donated by GGPP, rather than FPP. Other steps in the kinetic mechanism are identical.

FTase substrates in vivo include a number of important signaling molecules, including Ras-H, -N, -K4A, -K4B, and Rheb (*7*). Many of these protein substrates have been implicated in cancer progression; Ras, for example, is mutated in 30% of all human cancers (*8*). Thus, in the past decade, the pharmaceutical industry has developed FTase inhibitors (FTIs) that interfere with the FTase-catalyzed modification of both Ras and additional unidentified targets (*8*). GGTase I modifies the γ-subunits of most heterotrimeric G-proteins and many Ras-related G proteins, including

† This work was supported by National Institutes of Health Grant GM40602 (C.A.F.). Partial funding was also provided by Gaining Assistance in Areas of National Need Grant 037733 (H.L.H.), T32 GM07767 NIGMS (H.L.H.), and T32 GM08353 (K.A.H.) The contents of this publication are solely the responsibility of the authors and do not necessarily represent the official views of NIGMS.

* To whom correspondence should be addressed at 930 North University Avenue, Ann Arbor, MI 48109-1055. Phone, (734) 936-2678; fax, (734) 647-4865; e-mail, fierke@umich.edu.

‡ Department of Biological Chemistry, University of Michigan.

‖ Department of Chemistry, University of Michigan.

[1] Abbreviations: FTase, protein farnesyltransferase; FPP, farnesyl diphosphate; TCEP, tris(2-carboxyethyl)phosphine hydrochloride; I2, FPT Inhibitor II; Heppso, *N*-[2-hydroxyethyl]-piperazine-*N*′-[hydroxypropanesulfonic acid]; FRET, fluorescence resonance energy transfer; EDTA, (ethylenedinitrilo)tetraacetic acid; CaaX, tetrapeptide sequence cysteine−aliphatic amino acid−aliphatic amino acid−X; FTIs, farnesyltransferase inhibitors; GGTIs, geranylgeranyltransferase inhibitors; MDCC, the coumarin fluorophore *N*-[2-(1-maleimidyl)ethyl]-7-(diethylamino)coumarin-3-carboxamide; MEG, 7-methylguanosine; PNPase, purine nucleoside phosphorylase.

10.1021/bi050951v CCC: $30.25
Published on Web 10/29/2005

members of the Rac, Rap, and Rho families (*9*−*14*). Geranylgeranyltransferase inhibitors (GGTIs) inhibit human tumor growth and show promise in the treatment of cardiovascular disease (*15*). In general, peptide substrates of both FTase and GGTase I are proposed to contain a C-terminal Ca_1a_2X group, or "CAAX box", where C is a conserved cysteine residue, a_1 and a_2 are aliphatic amino acids, and X can be various amino acids (*1*, *16*, *17* (companion paper)). Many substrates also contain an upstream polybasic region, which has been proposed to increase the affinity of the protein substrate for the prenyltransferase, based on decreased IC_{50} values, and aid in plasma membrane localization (*18*−*20*). This region might also serve as a "second signal", allowing these protein substrates to be targeted directly to the plasma membrane from the endoplasmic reticulum rather than being trafficked through the Golgi (*21*). The classic structure of an upstream polybasic region is described by K-Ras4B, which has the sequence KKKKKKSKTKCVIM. However, there is no real consensus sequence for an upstream polybasic region, as some proteins (like K-Ras4B, RalA, and Rac1) contain stretches of positively charged amino acids, while other proteins (like G protein γ-T2 subunit and DnaJ) contain individually spaced Arg, Lys, or His residues (Table 1). The crystal structure of FTase with a bound K-Ras4B-derived peptide, $K_{11}K_{10}K_9S_8K_7T_6K_5C_4V_3I_2M_1$, indicates that numerous hydrogen-bonding interactions are made between the upstream lysines of this peptide with FTase residues. For example, Glu161α and Glu125α make backbone interactions with Lys7 and Lys10, respectively, Asp359β makes a side chain interaction with Lys5, and Asp91β hydrogen-bonds with Lys11 (*22*). Recent data indicate that the peptide substrate specificity of the prenyltransferases is more complex than originally proposed. Some substrates have dual specificity, that is, can be modified by either FTase or GGTase I. For example, K-Ras4B and RhoB are prenylated by both FTase and GGTase I (*7*, *24*−*26*). The differentially modified forms of these proteins may lead to resistance to FTIs and differential cellular effects (*27*, *28*). Here, we examine the effect of an upstream polybasic region, present in KRas-4B and RhoB, on reactivity with FTase and GGTase I. As predicted, our data demonstrate that the presence of an upstream polybasic region enhances the binding affinity of the peptide. However, the upstream polybasic region also decreases the apparent magnesium binding affinity and the farnesylation rate constant at saturating magnesium concentrations. These effects of the polybasic sequence lead to a *decrease* in the value of the specificity constant, $k_{cat}/K_M^{peptide}$, for reaction with FTase. In contrast, addition of a polybasic region has little effect on the reactivity or affinity of peptides with GGTase I. Therefore, these sequences enhance the dual specificity of these peptides by decreasing the value of $k_{cat}/K_M^{peptide}$ for farnesylation catalyzed by FTase relative to that of geranylgeranylation catalyzed by GGTase I.

EXPERIMENTAL PROCEDURES

Miscellaneous Methods. All curve fitting was performed with Kaleidagraph (Synergy Software, Reading, PA). Farnesyl protein transferase inhibitor II (I2) was purchased from Calbiochem-Novabiochem Corporation (San Diego, CA). The peptides used in these studies were synthesized and purified by HPLC to ≥90% pure, as follows: SKTKCVIM and TKCVIM, Bethyl Laboratories (Montgomery, TX); CCKVL, N-terminal-dansylated (dns) dns-KKKSKTKCVIM and dns-TKCVIM, Bio-Synthesis (Lewisville, TX); and KKKSKTKCVIM, KRYGSQNGCINCCKVL, and dns-SKTKCVIM, Sigma-Genosys (The Woodlands, TX). The concentration of peptide was determined spectroscopically by reaction of the cysteine thiol with 5,5′-dithio-bis(2-nitrobenzoic acid), using an ϵ_{412} of 14 150 M^{-1} cm^{-1} at 412 nm (*29*). Inorganic pyrophosphatase (PP_iase) from Bakers' Yeast, 7-methylguanosine (MEG), and purine nucleoside phosphorylase (PNPase) were all purchased from Sigma (St. Louis, MO). All other chemicals were reagent grade. Thin-layer chromatography (TLC) plates were pre-run in 100% acetone before use.

Preparation of FTase and GGTase I. Wild-type FTase was expressed in BL21(DE3) FPT/pET23a *Escherichia coli* and purified as described (*30*, *31*). The FTase concentration was determined by active site titration with dns-TKCVIM or dns-GCVLS as described (*31*). Wild-type GGTase I was expressed in BL21(DE3) GGPT/pET23a *E. coli* and purified, and the concentration was determined by active site titration as described (*2*, *17*). Purified FTase and GGTase I were determined by SDS−PAGE to be >90% pure. The proteins were dialyzed against HT buffer (50 mM 4-(2-hydroxyethyl)-1-piperazineethanesulfonic acid (Hepes), pH 7.8, and 1 mM tris(2-carboxyethyl)phosphine hydrochloride (TCEP)), concentrated to ∼100 μM, and stored at −80 °C.

Steady-State Kinetics. The steady-state kinetic constant $k_{cat}/K_M^{peptide}$ was measured for wild-type GGTase I using a continuous spectrofluorometric assay with dansylated peptides (*17*, *32*, *33*). Assays were performed at 25 °C in 50 mM Tris-HCl, pH 7.5, 5 mM dithiothreitol, 5 mM $MgCl_2$, and 10 μM $ZnCl_2$ with varying dansylated peptide (0.1−10 μM) and saturating GGPP (10 μM) (*33*). Additional enzyme (50−100 nM) was added to the reaction to reach the endpoint fluorescence (25−45 min). The rate of increase in fluorescence intensity per second was converted to the rate of increase in the product concentration per second using eq 1 where V refers to the velocity of the reaction (in μM s^{-1}), R refers to the velocity of the reaction (in fluorescence units s^{-1}), P refers to the concentration of the limiting substrate, and F_{max} refers to the maximal fluorescence intensity at the endpoint (*34*). The steady-state kinetic parameter $k_{cat}/K_M^{peptide}$ was calculated from the slope of the linear dependence of initial velocity on peptide concentration.

$$V = \frac{R \cdot P}{F_{max}} \quad (1)$$

This fluorescent assay was also used to measure the steady-state kinetics of FTase with the peptides dns-KKKSKTKCVIM, dns-SKTKCVIM, and dns-TKCVIM. The reactions contained 0.1−3 μM peptide, 10 μM FPP, 0−10 mM $MgCl_2$, 50 mM Heppso−NaOH, pH 7.8, 5 mM TCEP, 10 μM $ZnCl_2$, and 24 nM FTase. The Michaelis−Menten equation was fit to the initial velocity data to generate values of $k_{cat}/K_M^{peptide}$ and $K_M^{peptide}$ at 5 mM $MgCl_2$. The dependence of $k_{cat}/K_M^{peptide}$ on $MgCl_2$ was also measured to determine values for $k_{cat}/K_{M,Mg}$ and $K_{M,Mg}$.

The steady-state parameter $k_{cat}/K_M^{peptide}$ was determined for FTase with the peptides SKTKCVIM, TKCVIM, KRYGSQNGCINCCKVL, and CCKVL using a radioactive assay

(*17*, *31*). Assays were initated by the addition of FTase to peptide and FPP. The final concentrations were 24 nM FTase; 1 μM [1-^{3}H]FPP and 0.1−4 μM peptide in 50 mM Heppso−NaOH, pH 7.8, and 5 mM $MgCl_2$; and 2 mM TCEP, pH 7.8. Reactions were quenched by the addition of an equal volume of 20% (v/v) acetic acid/80% 2-propanol. The product was separated by TLC and quantified by scintillation counting. The initial rate, v_0, at each peptide concentration was calculated from a linear fit of the first 10% of the reaction. The slope of the dependence of v_0/[E] on the peptide concentration yields the $k_{cat}/K_M^{peptide}$ values.

Direct Peptide Binding Affinity. The binding of dansylated peptides to FTase and GGTase I was observed by fluorescence anisotropy (*17*, *35*). The FTase (0.5 nM) samples were prepared with 50 mM Heppso, pH 7.8, 2 mM TCEP, 1 mM $MgCl_2$, 57 mM NaCl, and 0.2 nM EDTA; in some cases, 1 nM I2, an FPP analogue, was also included in the sample. Dansylated peptide (0−12 nM) was then titrated into the enzyme solution, and the fluorescence anisotropy was measured. The GGTase I titrations contained 50 mM Heppso, pH 7.8, 2 mM TCEP, 2 nM dansylated peptide, and 10 nM EDTA. GGTase I:3-aza-GGPP was then titrated into solution (0−150 nM) and additional dansylated peptide to maintain the 2 nM concentration of peptide. A weighted fit of eq 2 to the data yields the apparent dissociation constants, where ΔA corresponds to the observed fluorescence anisotropy (excitation, 340 nm; emission, 496 nm), EP is the fluorescence anisotropy endpoint, IF is the initial fluorescence anisotropy, [enzyme] is the concentration of FTase, and $K_D^{peptide}$ is the dissociation constant for the dansylated peptide.

$$\Delta A = \frac{EP}{1 + K_D^{peptide}/[enzyme]} + IF \quad (2)$$

Transient Kinetics. Single turnover rate constants for FTase and GGTase I were determined using a coupled stopped-flow fluorescence assay with fluorophore-labeled phosphate binding protein to measure the formation of phosphate, in the presence of inorganic pyrophosphatase, as described (*17*, *36*). Briefly, a mixture of 1.6 μM FTase or GGTase I, 0.4 μM FPP or GGPP, 50 mM Heppso, pH 7.8, 0.01−50 mM $MgCl_2$, 2 mM TCEP, and a "phosphate mop" was mixed in a stopped-flow apparatus (KinTek Corporation, Austin, TX) with an equal volume of peptide (0.02−0.4 mM), 0.01 mM MDCC-labeled A197C PBP, 100 μL/mL PPiase, 50 mM Heppso, 1 mM TCEP, and "phosphate mop". The "phosphate mop", composed of 0.5 units/mL purine nucleoside phosphorylase (PNPase) and 15 mM 7-methylguanosine (MEG), was added to remove any contaminating phosphate present in the reaction mixture. Eq 3 was fit to these data to calculate k_{chem} values. Fl refers to the observed fluorescence (em = 450 nm), amp represents the amplitude of the fluorescence change (em = 450 nm), k_{chem} represents the rate constant for formation of monophosphate (which equals the prenylation rate constant), and IF is the initial fluorescence.

$$Fl = amp[1 - \exp(-k_{chem}t)] + IF \quad (3)$$

The magnesium dependence of the farnesylation reaction was determined by varying the magnesium concentration from 0.01 to 50 mM and measuring the single turnover rate constant using the phosphate binding protein stopped-flow assay. Eq 4 was fit to these data. K_{Mg} represents the apparent dissociation constant for magnesium, k_{max}^{Mg} is the rate constant of the reaction at saturating magnesium concentration, and k_0 is the rate constant of the reaction in the absence of magnesium.

$$k_{obs} = \frac{k_{max}^{Mg}}{1 + K_{Mg}/[Mg^{2+}]} + k_0 \quad (4)$$

Table 1: Selected Prenylated Proteins Containing an Upstream Polybasic Region[a]

protein	C-terminal sequence	modification
Rac1	CPPPV**KKRKRK**CLLL	geranylgeranylated
RalA	**KKKRK**SLA**KRIRER**CCIL	geranylgeranylated
R-Ras	AP**RKK**GGGCPCVLL	geranylgeranylated
Guanine nucleotide binding protein G(1)/G(S)/G(O) gamma-11 subunit	**K**NPF**K**E**K**GSCVIS	farnesylated
DnaJ	EDDE**HH**P**R**GGVQCQTS	farnesylated
PRL-1 (PTPCAAX1)	**K**DSNG**HR**NNCCIQ	farnesylated
G protein, γ-T2 subunit	D**K**NPF**K**E**K**GGCLIS	farnesylated
K-Ras4B	**KKKKKK**S**K**T**K**CVIM	both
RhoB	**KR**YGSQNGCINCCKVL	both

[a] Data taken from the Swiss-Prot databank and refs *20* and *21*.

RESULTS

A number of prenyltransferase substrates contain positively charged amino acids on the N-terminal side of the CaaX sequence, such as K-Ras4B, RalA, Rac1, G protein γ-T2 subunit, and Dna J (Table 1) (*20*, *21*). This region is proposed to act as a "second signal", allowing these proteins to be targeted directly to the plasma membrane rather than being trafficked through the Golgi (*21*). This sequence is also proposed to increase the binding affinity of FTase for these substrates, as suggested by a decrease in the steady-state K_M (*38*). In addition, peptides based on the C-terminal region of K-Ras4B have IC_{50} values for inhibition of farnesylation in the high-nanomolar regime, and farnesylation of K-Ras4B exhibits resistance to FTIs (*19*, *20*). However, peptide dissociation constants and chemical rate constants catalyzed by the protein prenyltransferases cannot be directly determined using steady-state kinetics (*3*, *5*).

Here, we investigate the molecular recognition and function of interactions between FTase or GGTase I and positively charged upstream amino acids in a series of peptides using single turnover and steady-state kinetics and direct binding assays. The reactivity and affinity of peptides based on two proteins that are prenylated by both FTase and GGTase I (Table 1), K-Ras4B (KKKSKTKCVIM, SKTKCVIM, and TKCVIM), and Rho B (KRYGSQNGCINCCKVL and CCKVL) are examined (*7*).

Polybasic Region Decreases Selectivity for FTase. The steady-state parameters $k_{cat}/K_M^{peptide}$ and k_{cat} were measured for a series of peptides based on the protein substrates with and without upstream polybasic sequences (Tables 2 and 3). The addition of an upstream polybasic region decreases the value of k_{cat} modestly (2-fold) for the peptide KKKSKTKCVIM in comparison to TKCVIM. However, the value of

Table 2: Kinetic Constants of FTase and GGTase I with K-Ras4B Peptides

	dns-KKKSKTKCVIM	dns-SKTKCVIM	dns-TKCVIM
FTase			
$k_{cat}/K_M^{peptide}$ ($mM^{-1}\,s^{-1}$)[a,b] (5 mM Mg)	2.7 ± 0.7	80 ± 8	16 ± 2
k_{cat} (s^{-1})[a,b]	0.052 ± 0.008	0.20 ± 0.04	0.096 ± 0.008
$k_{cat}/K_M^{peptide}$ ($mM^{-1}\,s^{-1}$)[a,c] (saturating Mg)	10 ± 1[i]	82 ± 5	41 ± 3
$K_{M,Mg}$ (μM)[a,c]	13 ± 3	100 ± 10	24 ± 6
$K_D^{peptide}$ (nM)[d]	0.14 ± 0.03	0.22 ± 0.03	0.86 ± 0.08
k_{chem} (s^{-1}) (5 mM Mg)[b,e]	1.1 ± 0.1	0.92 ± 0.09	7.3 ± 0.7
K_{Mg} (mM)[e,f]	11 ± 1	11 ± 1	2.2 ± 0.2
k_{max} (s^{-1})[e,f,g] saturating Mg	3.3 ± 0.3	3.4 ± 0.3	9 ± 3
k_0 (s^{-1})[h]	0.029 ± 0.003	0.023 ± 0.002	0.24 ± 0.03
GGTase I			
$k_{cat}/K_M^{peptide}$ ($mM^{-1}\,s^{-1}$)[a]	20 ± 1	21 ± 1	16 ± 1
$K_D^{peptide}$ (nM)[d,i]	1.0 ± 0.4	2.0 ± 0.9	3 ± 1
k_{chem} (s^{-1})[e]	0.94 ± 0.01	0.34 ± 0.06	0.35 ± 0.02

[a] Assays were performed with saturating FPP or GGPP at pH 7.8 with dansylated peptides. [b] Measured at 5 mM $MgCl_2$. [c] Both $k_{cat}/K_{M,Mg}$ and $K_{M,Mg}$ are kinetic parameters determined from the magnesium dependence of $k_{cat}/K_M^{peptide}$ at saturating FPP. [d] Measured from fluorescence changes of dansylated peptides. [e] Single turnover assays were measured at pH 7.8 with saturating enzyme and peptide. [f] The single turnover rate constant was measured as a function of Mg(II) concentration. [g] Saturating Mg(II). [h] Single turnover rate constant at zero Mg(II). [i] Binding assay done in the presence of the non-hydrolyzable analogue 3-aza-GGPP. [i] Value calculated using $[Mg^{2+}] < 0.7$ mM since $k_{cat}/K_M^{peptide}$ decreases at higher concentrations.

Table 3: Kinetic Constants for Farnesylation of Peptides Based on RhoB

FTase	KRYGSQNGCINCCKVL	CCKVL
k_{chem} (s^{-1})[a]	0.44 ± 0.04	1.1 ± 0.1
$k_{cat}/K_M^{peptide}$ ($mM^{-1}s^{-1}$)[b]	48 ± 6	70 ± 10

[a] Single turnover assays were measured at pH 7.8 with saturating enzyme and peptide. [b] Steady-state kinetics measured using the radioactive multiple turnover assay.

$k_{cat}/K_M^{peptide}$ is the most relevant kinetic parameter since it reflects the specificity constant under steady state turnover, indicating which peptide is most likely to be prenylated under steady-state conditions when in competition with other substrates, as would be seen in vivo (*37*). Our data demonstrate that addition of lysines at the N-terminus (KK_{10}-$KSKTK_5CVIM_1$ versus $SKTK_5CVIM_1$) decreases the value of $k_{cat}/K_M^{peptide}$ by 30-fold at 5 mM $MgCl_2$, specifically reducing the specificity of FTase for catalyzing farnesylation of the peptide with the polybasic region. Similar results were obtained with nondansylated peptides using a radioactive assay (data not shown). In contrast, previous comparisons of farnesylation of the full-length proteins N-Ras (-QGCMGLPCVVM), K-Ras4A (-GCVKIKKCIIM), and K-Ras4B (-KKKSKTKCVIM) catalyzed by human FTase demonstrated that K-Ras4B had the highest value of $k_{cat}/K_M^{protein}$ and lowest value of K_M (*38*). The authors concluded that the polybasic region enhances catalytic efficiency of this substrate; however, our data suggest that these two effects may be caused by the sequence changes at the a_1 and a_2 position of the CaaX sequence rather than the upstream sequence. Alternatively, the differential results could be caused by the lower concentration of FPP (0.5 μM versus 10 μM) in the previous work or the use of full-length proteins. In summary, our data demonstrate that the catalytic efficiency for farnesylation of peptides catalyzed by rat FTase *decreases* with the addition of an upstream polybasic sequence.

In contrast, the specificity constants for farnesylation of KRYGSQNGCINCCKVL and CCKVL are nearly identical, likely reflecting the absence of specific interactions between the amino acids immediately upstream (amino acids 5−12) of the CAAX box (Table 3), including positively charged residues. The high reactivity of the peptides based on K-Ras4B (Table 2) is not unexpected as this protein is farnesylated in vivo. However, the comparable values of $k_{cat}/K_M^{peptide}$ for the reaction of FTase with the RhoB peptides, where the terminal amino acid ("X") is Leu (-CCKVL), is surprising given the low specificity rate constant ($k_{cat}/K_M^{peptide} < 10^1\ M^{-1}\ s^{-1}$) previously measured for the TKCVIL peptide (*17*). The data in Table 3 demonstrate that the enhanced reactivity of the RhoB peptide with FTase is not caused by the upstream polybasic sequence. Therefore, changes in the YCa_1a_2X sequence, such as Lys at a_1, Ile at a_2, or Cys at Y, must enhance the reactivity of this peptide with FTase.

For GGTase I, the presence of an upstream polybasic region has a limited effect on the value of $k_{cat}/K_M^{peptide}$ for the K-Ras4B peptide series (Table 2); dns-KKKSKTKCVIM, dns-SKTKCVIM, and dns-TKCVIM have nearly identical values of $k_{cat}/K_M^{peptide}$ ($16-20\ mM^{-1}\ s^{-1}$). Thus, upstream polybasic regions have little effect on the specificity of geranylgeranylation catalyzed by GGTase I. A similar conclusion has been previously reached for geranylgeranylation of peptides catalyzed by "humanized" rat GGTase I (*38*). Taken together, these data indicate that upstream polybasic residues alter the partitioning of a given peptide toward geranylgeranylation by GGTase I compared to farnesylation by FTase. This ratio, indicated by $(k_{cat}/K_M^{peptide})^{GGTase}/(k_{cat}/K_M^{peptide})^{FTase}$, increases from 0.3 for TKCVIM to 7.4 for KKKSKTKCVIM, suggesting that, in the presence of equal concentrations of GGTase·GGPP and FTase·FPP, TKCVIM would be predominantly (~80%) farnesylated while KKKSKTKCVIM would be mainly geranylgeranylated (~90%). Thus, the upstream polybasic region in the K-Ras4B peptide modulates the dual specificity of this peptide. Interestingly, although methionine at the C-terminus has been suggested as a determinant of reactivity with FTase, the K-Ras4B peptides are efficient substrates for GGTase I with $k_{cat}/K_M^{peptide}$ values comparable to both the reaction of GGTase I with peptides where X = L (Tables 2 and 3) and reactivity of FTase with peptides where X = M (Table 2) (*17*).

The partitioning between farnesylation and geranylgeranylation of a given peptide is also altered by the magnesium concentration since FTase, but not GGTase I, is activated by magnesium (*2*, *40*). To investigate whether upstream polybasic residues affect the magnesium dependence of FTase, the dependence of $k_{cat}/K_M^{peptide}$ on the concentration of magnesium was measured for the peptides KKKSKTKCVIM, SKTKCVIM, and TKCVIM (Table 2) (Figure 2). The value of $K_{M,Mg}$ is calculated from the dependence of $k_{cat}/K_M^{peptide}$ on the concentration of magnesium and likely

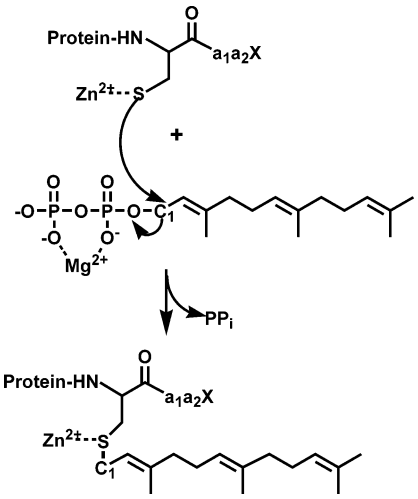

FIGURE 1: The overall reaction catalyzed by FTase. A thioether bond is formed between Carbon 1 (C1) of FPP and the Cys thiolate of the CAAX box. For FTase, Mg^{2+} is known to enhance the rate constant of chemistry, while GGTase I catalysis is magnesium-independent. The chemical reaction catalyzed by GGTase I is nearly identical, except that a 20-carbon group is attached to the Cys thiolate of the CAAX box, which is donated from GGPP.

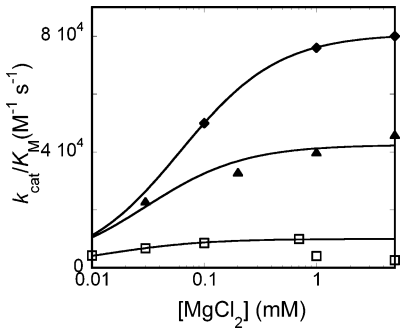

FIGURE 2: The dependence of $k_{cat}/K_M^{peptide}$ on the magnesium concentration was determined for the peptides dns-TKCVIM (▲), dns-SKTKCVIM (◆), and dns-KKKSKTKCVIM (□). The value of $k_{cat}/K_M^{peptide}$ was measured using the continuous fluorescent assay (see Experimental Procedures) under standard conditions with varying concentrations of Mg(II). The Michaelis−Menten equation was fit to these data yielding $K_{M,Mg}$ and $k_{cat}/K_M^{peptide}$ at saturating $MgCl_2$ (Table 2).

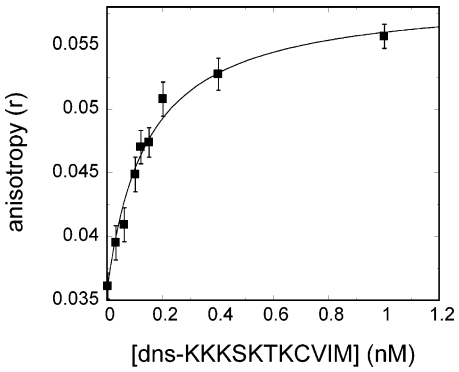

FIGURE 3: Measurement of K_d for the FTase·dns-KKKSKTKCVIM complex using changes in the fluorescence anisotropy. The solution anisotropy was measured as the peptide dns-KKKSKTKCVIM was titrated into 0.2 nM FTase as described in Experimental Procedures. Equation 2 was fit to these data to calculate a value of K_d.

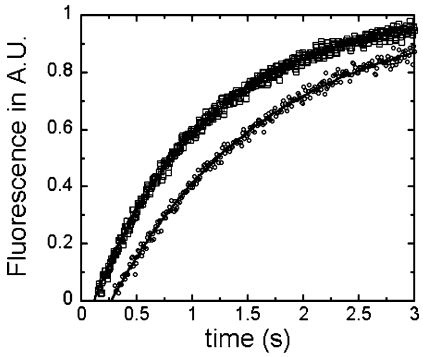

FIGURE 4: The single turnover rate constant for prenylation of KKKSKTKCVIM. Prenylation of KKKSKTKCVIM catalyzed by FTase (○) and GGTase I (□) was measured using the stopped-flow assay. The peptide KKKSKTKCVIM was mixed with enzyme in a KinTek stopped-flow at the following concentrations: saturating peptide (20 μM) and either 1.6 μM FTase or GGTase I, in 0.4 μM FPP or GGPP, 50 mM Heppso, pH 7.8, 2.5−5 mM $MgCl_2$, 2 mM TCEP, 0.5 units/mL PNPase, 15 mM MEG, 100 μL/mL PPiase, and 0.01 mM MDCC-labeled A197C PBP. The increase in phosphate concentration was measured fluorometrically by binding to MDCC-labeled A197C PBP, as described in Experimental Procedures. Equation 3 was fit to these data to obtain values for k_{chem}.

does not directly measure the binding affinity for magnesium. The value of $K_{M,Mg}$ increases with the addition of one upstream lysine from 24 to 100 μM, while additional lysines cause a decrease in $K_{M,Mg}$. For peptides with multiple upstream lysines, the value of $k_{cat}/K_M^{peptide}$ decreases at concentrations of $MgCl_2$ above 0.7 mM. These data demonstrate that the upstream polybasic residues alter the dependence of $k_{cat}/K_M^{peptide}$ on the concentration of $MgCl_2$.

Polybasic Region Enhances Binding Affinity for FTase. To further investigate the role of the upstream polybasic region, we measured the binding affinity of FTase and GGTase I for a number of peptides. As predicted, the addition of upstream lysine residues increases the affinity of a peptide for FTase 3−4-fold, as indicated by a comparison of the K_D values for dns-KKKSKTKCVIM with that of dns-TKCVIM (Figure 3). The presence of an upstream region also has a modest effect on the affinity of GGTase I for peptides, increasing the affinity of K-Ras4B-derived peptides by 2-fold (Table 2). However, FTase binds K-Ras4B-derived peptides with 4−9-fold higher affinity than GGTase I. This increase in binding affinity for FTase is not observed as an increase in the $k_{cat}/K_M^{peptide}$ for FTase; rather, the specificity constant decreases (Table 2). This result demonstrates that the binding affinity of a peptide does not correlate with reactivity for FTase.

Lysines Decrease Prenylation Rate Constant and Magnesium Affinity. To further understand the effects of the upstream polybasic residues on catalysis, the rate constant for farnesylation or geranylgeranylation was measured under single turnover conditions (Figure 4). Unexpectedly, upstream polybasic residues in the K-Ras4B peptide series cause a significant decrease (7-fold) in the farnesylation rate constant catalyzed by FTase at 5 mM $MgCl_2$ (Table 2). This effect is mediated by the upstream lysine residue at position 7, as the measured rate constants for SK_7TKCVIM and KKKSK_7TKCVIM are nearly identical and slower than TKCVIM. The addition of an upstream sequence lacking this lysine, as in the peptide KRYGSQNGCINCCKVL (Table 3), has a smaller effect on k_{chem} consistent with this conclusion. To investigate whether the lysine residues also affect the apparent magnesium affinity of the FTase·FPP·

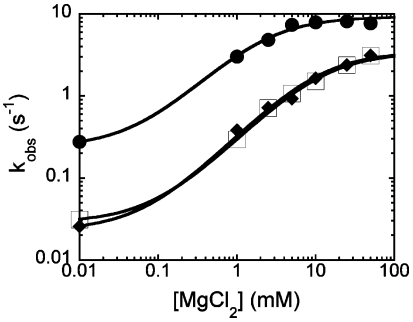

FIGURE 5: The single turnover rate constant for the peptides TKCVIM (●), SKTKCVIM (◆), and KKKSKTKCVIM (□) was measured using the stopped-flow PBP assay (as described in the legend of Figure 3) at varying magnesium concentrations (0.01−50 mM). Equation 4 was fit to these data to determine K_{Mg} (Table 2).

peptide ternary complex, the single turnover rate constant was measured at varying concentrations of magnesium to measure K_{Mg}. Magnesium ions accelerate the single turnover rate constant for farnesylation of GCVLS catalyzed by FTase 700-fold with a K_{Mg} of 2 mM (*3*, *42*). Magnesium ions are proposed to coordinate to the diphosphate of FPP, leading to stabilization of the diphosphate leaving group in the transition state for farnesylation (*42*). The measured value of K_{Mg} for farnesylation of TKCVIM catalyzed by FTase is 2.2 ± 0.1 mM (Figure 5), nearly identical to the value of K_{Mg} determined for GCVLS. Therefore, the lysine adjacent to the CAAX box does not alter the apparent Mg(II) affinity. The value of K_{Mg} is much higher than the value of $K_{M,Mg}$ determined from the magnesium dependence of $k_{cat}/K_M^{peptide}$ (Table 2), since the latter value reflects the concentration of Mg(II) required to change the rate-limiting step from a Mg(II)-dependent step, such as farnesylation, to a Mg(II)-independent step, such as peptide association. However, addition of a lysine residue at position 7 (SK_7TKCVIM) decreases both the apparent Mg(II) affinity 5-fold (K_{Mg} = 11 ± 1 mM) and the farnesylation rate constant at saturating Mg(II) by 2−3-fold (Table 2). In the absence of Mg(II), addition of a lysine at position 7 in the peptide also decreases the farnesylation rate constant by ~10-fold. Additional upstream lysine residues, as in the peptide KKKSKTKCVIM, have little affect on the value of k_{max}, k_0, or K_{Mg} measured at pH 7.8. These data demonstrate that a lysine at position 7 from the C-terminus decreases both the farnesylation rate constant and the magnesium affinity, while modestly enhancing $k_{cat}/K_M^{peptide}$ (Table 2).

In contrast to FTase, the presence of an upstream polylysine region modestly increases the magnitude of the chemical rate constant catalyzed by GGTase I in the K-Ras4B peptide series. For example, KKKSKTKCVIM has the largest value of k_{chem} (0.94 s^{-1}), while the value of this rate constant is decreased ~3-fold for peptides with fewer upstream basic residues, including SKTKCVIM and TKCVIM. However, this increase in k_{chem} is not reflected as an increase in $k_{cat}/K_M^{peptide}$, further demonstrating that geranylgeranylation is not rate-limiting under these conditions.

DISCUSSION

Effects of the Polybasic Region on Binding and Catalysis. KRas-4B is often mutated in human cancers; thus, there is great interest in inhibiting prenylation of this protein.

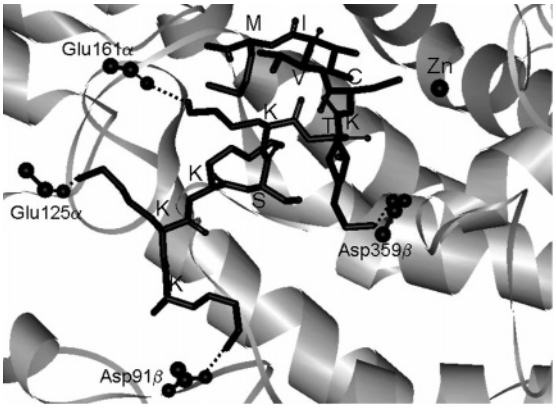

FIGURE 6: Crystal structure of FTase complexed with the peptide $K_{11}K_{10}K_9S_8K_7T_6K_5C_4V_3I_2M_1$ (PDB ID18D8). Highlighted are the backbone interactions between Glu161α and Glu125α and Lys7 and Lys10, respectively. In addition, side chain interactions are made between Asp359*β* and Lys5 and also between Asp91*β* and Lys11 (*22*).

However, KRas-4B has been shown to be largely resistant to FTIs presumably because it has a low K_M for FTase and can be alternatively prenylated by GGTase I (*7*). On the basis of the crystal structure of KKKSKTKCVIM bound to FTase, hydrogen-bonding interactions are made between the upstream lysine region of $K_{11}K_{10}K_9S_8K_7T_6K_5C_4V_3I_2M_1$ with negatively charged Glu and Asp residues on FTase (Figure 6). For example, Glu161α and Glu125α interact with the backbone of Lys7 and Lys10, respectively. Asp359*β* makes a side chain interaction to Lys5, and Asp91*β* hydrogen-bonds to the side chain of Lys11 (*22*). Our data demonstrate that the addition of the upstream lysine residues to the KRas4B peptide increases the binding affinity by 0.75 kcal/mol, which is less than the energy of forming one or more buried salt bridges, but comparable to the energy of forming two or more solvent-exposed salt bridges (0.1−0.5 kcal mol^{-1} each) (*37*). However, each lysine has a modest effect; Lys7 causes the largest enhancement, increasing binding affinity by 0.54 kcal mol^{-1}. Thus, the enhanced binding affinity observed for the K-Ras4B peptide is likely due to a solvent-exposed salt bridge formed between Lys7 and Glu161α in FTase as well as the formation of several other weak hydrogen bonds.

Interactions between an enzyme and a substrate often cause an increase in catalytic activity as well as enhanced binding (*17*, *37*). However, our data indicate that the presence of an upstream polybasic region leads to decreases in the $k_{cat}/K_M^{peptide}$ for farnesylation. Since farnesylation followed by rapid diphosphate release (*36*) is an irreversible step, the steady-state parameter $k_{cat}/K_M^{peptide}$ includes the rate constants for the steps from peptide binding to E·FPP through farnesylation. Crystallographic data suggest that, prior to the actual farnesylation step, the prenyl chain of FPP rotates in the FTase·FPP·peptide complex to position the C1 of FPP near the sulfur nucleophile in the peptide (*22*, *44*). Therefore, the decrease in $k_{cat}/K_M^{peptide}$ observed for the peptides containing a polybasic region could reflect decreases in the rate constant for peptide association, prenyl chain rotation, and/or the farnesylation step (Scheme 1). The observed decreases in the single turnover rate constant for farnesylation (k_{chem}) likely partially explain the decreases in $k_{cat}/K_M^{peptide}$. However, at 5 mM magnesium, the decrease in $k_{cat}/K_M^{peptide}$ caused by the addition of an upstream polybasic region is

significantly larger than the decrease in k_{chem} (Table 2). Therefore, a decrease in the peptide association rate constant and/or alteration of the partitioning of the FTase·FPP·peptide complex between peptide dissociation and farnesylation must also play a role in the decreased specificity constant. Alterations in the association rate constant could be related to changes in the peptide conformation required to form interactions between the upstream polybasic region and FTase (Figure 6) that are observed crystallographically (*22*). Although dissociation of the farnesylated product is the rate-limiting step under k_{cat} conditions (*5*), this step is not expected to affect substrate selectivity as it occurs after the first irreversible step. The addition of the upstream polybasic region also decreases the product dissociation rate constant modestly (2-fold); this effect is similar to the increase in substrate binding affinity (~3.5-fold).

Additionally, the presence of an upstream polybasic region leads to decreases in the single turnover rate constant for farnesylation (k_{chem}), both in the absence of magnesium and in the presence of saturating levels of magnesium (k_0 and k_{max}), as well as an apparent decrease in the affinity of Mg(II) (K_{Mg}). These decreases in the apparent magnesium affinity and activity could be a direct electrostatic effect whereby the polylysine region increases the overall positive charge of the active site and inhibits the affinity of the positively charged Mg(II) ion while destabilizing the developing positive charge on C1 in the transition state (*3*). Alternatively, the magnesium affinity may be linked to the bound conformation of FPP. A crystal structure of an inactive FTase·FPP·peptide complex indicates that the C1 of FPP is more than 7 Å away from the nucleophile sulfur of the peptide (*22*). The structure of the FTase·farnesyl-peptide complex indicates that the prenyl chain rotates to form the C1−S bond (*44*). Therefore, a similar conformation change in FPP likely occurs prior to catalysis and this step may be important for regulating the farnesylation rate constant. Asp352β is proposed to be a magnesium ligand in the FTase-catalyzed reaction based on the decrease in Mg(II) affinity when Asp352β is changed to Ala or Lys (4). However, in the structures of FPP bound to FTase, the side chain of Asp352β is >7 Å from the diphosphate of FPP. In the modeled active ternary complex, an octahedral Mg(II) site is proposed to form including as ligands two nonbridging oxygens of the diphosphate, the two carboxylate oxygens of Asp352β, a water molecule, and one carboxylate oxygen of Asp297β (4). Therefore, Mg(II) binding could be linked to formation of the active conformation. The crystal structure of the "full length" KRas-4B peptide bound to FTase shows that the side chain of Lys5 in the peptide is >7 Å from the side chain of Asp352β in the ground state, ruling out a direct effect of this side chain on Mg(II) affinity. However, the presence of the upstream polybasic region could stabilize the FPP molecule in the inactive conformation, leading to a lowered farnesylation rate constant in the absence of Mg(II) (k_0 decreases 10-fold). Given the coupling between Mg(II) binding and the formation of the active complex, stabilization of the inactive conformation should also increase the concentration of Mg(II) required to shift the complex into the active form and, hence, increase the value of K_{Mg}, as observed. Furthermore, the reactivity of the peptide with a polybasic region remains lowered at saturating magnesium. These changes in the observed single turnover rate constant could either reflect a decrease in the reactivity of the active conformation **or** a decrease in the concentration of the active complex at saturating Mg(II) (Scheme 2).

Scheme 2: Proposed Coupling between Mg(II) Binding and Formation of the Active Complex in FTase[a]

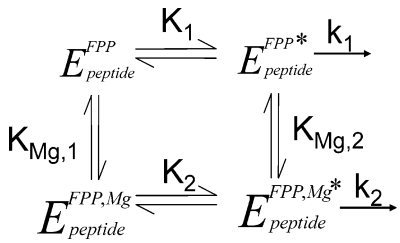

[a] The polybasic peptides are proposed to stabilize the inactive $E^{FPP}_{Peptide}$ and $E^{FPP,Mg}_{peptide}$ conformations, relative to the active FPP conformation, leading to decreased observed values of k_0 and k_{max} and an increased value of K_{Mg} assuming that there is a rapid equilibrium between the four forms. This model also assumes that $K_{Mg,2} < K_{Mg,1}$ leading to $K_2 > K_1$.

Scheme 3: The Upstream Polybasic Region Mediates Partitioning between FTase and GGTase I

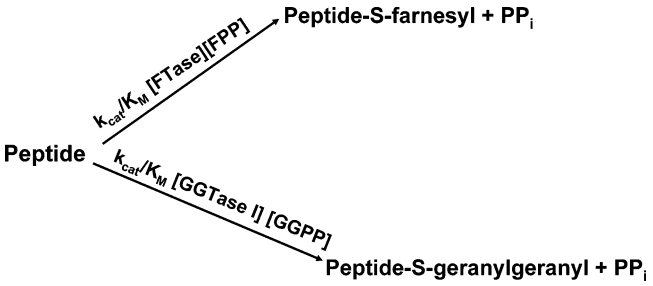

In contrast, the presence of upstream polybasic residues has a more limited effect on GGTase I catalysis and binding with only a 2-fold effect on K_D and a 3-fold effect on k_{chem}. This is not entirely unexpected, as the amino terminal substrate residues were not observed in the electron density of the crystal structure of KKKSKTKCVIL bound to GGTase I (*23*). This suggests that no specific binding interactions occur. In general, in the GGTase I-catalyzed reaction, the presence of upstream polybasic content modestly increases binding affinity and specificity constants.

Biological Implications. The data presented here indicate that the upstream polybasic region can modulate the FTase/GGTase I selectivity of a protein substrate by decreasing the $k_{cat}/K_M^{peptide}$ for farnesylation leading to a net enhancement of geranylgeranylation (Scheme 3). Therefore, the polybasic sequence may be an important molecular recognition feature that signals dual specificity of a peptide for reaction with both FTase and GGTase I. Furthermore, the upstream polybasic region alters the apparent magnesium affinity of FTase, perhaps allowing for in vivo regulation of prenylation rates and selectivity of the prenyl donor by changes in the magnesium concentration. For example, it is possible that, when magnesium concentration is low, GGTase I preferentially modifies K-Ras4B, whereas, at higher Mg(II) concentrations, this protein is farnesylated. Biologically, the distinction between a geranylgeranylated versus farnesylated version of a protein could have different effects. Recent work, for example, indicates that geranylgeranylated RhoB suppresses Ras transformation in NIH-3T3 cells, while farnesylated RhoB does not (*45*). In vivo, magnesium is sequestered by ATP, and thus, regulation of the differential prenylation

of substrates could involve delicate coordination of both ATP and magnesium levels leading to divergent downstream effects (*41*).

ACKNOWLEDGMENT

We thank Andrea Stoddard for construction of the A197C PBP plasmid.

REFERENCES

1. Zhang, F. L., and Casey, P. J. (1996) Protein prenylation: Molecular mechanisms and functional consequences, *Annu. Rev. Biochem. 65*, 241−269.
2. Hartman, H. L., Bowers, K. E., and Fierke, C. A. (2004) Lysβ311 of protein geranylgeranyltransferase type I partially replaces magnesium, *J. Biol. Chem. 279*, 30546−30553.
3. Huang, C. C., Hightower, K. E., and Fierke, C. A. (2000) Mechanistic studies of rat protein farnesyltransferase indicate an associative transition state, *Biochemistry 39*, 2593−2602.
4. Pickett, J. S., Bowers, K. E., and Fierke, C. A. (2003) Mutagenesis Studies of protein farnesyltransferase implicate aspartate β352 as a magnesium ligand, *J. Biol. Chem. 278*, 51243−51250.
5. Furfine, E. S., Leban, J. J., Landavazo, A., Moomaw, J. F., and Casey, P. J. (1995) Protein farnesyltransferase: Kinetics of farnesyl pyrophosphate binding and product release, *Biochemistry 34*, 6857−6862.
6. Tschantz, W. R., Zhang, L., and Casey, P. J. (1999) Cloning, expression, and cellular localization of a human prenylcysteine lyase, *J. Biol. Chem. 274*, 35802−35808.
7. Cox, A. D., and Der, C. J. (1997) Farnesyltransferase inhibitors and cancer treatment: targetting simply Ras?, *Biochim. Biophys. Acta 1333*, F51−F71.
8. Cox, A. D. (2001) Farnesyltransferase inhibitors: Potential role in the treatment of cancer, *Drugs 61*, 723−732.
9. Kawata, M., Farnsworth, C. C., Yoshida, Y., Gelb, M. H., and Takai, Y. (1990) Posttranslationally processed structure of the human platelet protein smg p21B: Evidence for geranylgeranylation and carboxyl methylation of the C-terminal cysteine, *Proc. Natl. Acad. Sci. U.S.A. 87*, 8960−8964.
10. Mumby, S. M., Casey, P. J., Gilman, A. G., and Sternweis, P. C. (1990) G proteins γ subunits contain a 20-carbon isoprenoid, *Proc. Natl. Acad. Sci. U.S.A. 87*, 5873−5877.
11. Tamanoi, F., Gau, C. L., Jiang, C., and Kato-Stankiewicz, J. (2001) Protein farnesylation in mammalian cells: Effects of farnesyltransferase inhibitors on cancer cells, *Cell. Mol. Life Sci. 58*, 1636−1649.
12. Yamane, H. K., Farnsworth, C. C., Xie, H. Y., Evans, T., Howald, W. N., Gelb, M. H., Glomset, J. A., and Fung, B. K. (1991) Membrane-binding domain of the small G protein G25K contains an *S*-(all-*trans*-geranylgeranyl) cysteine methyl ester at its carboxyl terminus, *Proc. Natl. Acad. Sci. U.S.A. 88*, 286−290.
13. Casey, P. J. (1994) Lipid modifications of G proteins, *Curr. Opin. Cell Biol. 6*, 219−225.
14. Maltese, W. A. (1990) Posttranslational modification of proteins by isoprenoids in mammalian cells, *FASEB J. 4*, 3319−3328.
15. Sebti, S. M., and Hamilton, A. D. (2001) Farnesyltransferase Inhibitors in Cancer Therapy, in *Cancer Drug Discovery and Development* (Teicher, B. A., Ed.)Vol. 8, Humana Press, Totowa, NJ.
16. Boutin, J. A., Marande, W., Petit, L., Loynel, A., Desmet, C., Canet, E., and Fauchere, J. L. (1999) Investigations of *S*-farnesyl transferase substrate specificity with combinatorial tetrapeptide libraries, *Cell. Signalling 11*, 59−69.
17. Hartman, H. L., Hicks, K. A., and Carol A. Fierke. (2005) Peptide specificity of protein prenyltransferases is determined mainly by reactivity rather than binding affinity, *Biochemistry*, *44*, 15314−15324.
18. Apolloni, A., Prior, M., Lindsay, P. R. G., and Hancock, J. F. (2000) H-ras but not K-ras traffics to the plasma membrane through the exocytic pathway, *Mol. Cell. Biol. 20*, 2475−2487.
19. James, G. L., Goldstein, J. L., and Brown, M. S. (1995) Polylysine and CVIM sequences of K-RasB dictate specificity of prenylation and confer resistance to benzodiazepine peptidomimetic *in vitro*, *J. Biol. Chem. 270*, 6221−6226.
20. Fiordalisi, J. J., Johnson, R. L., II, Weinbaum, C. A., Sakabe, K., Chen, Z., Casey, P. J., and Cox, A. D. (2003) High affinity for farnesyltransferase and alternative prenylation contribute individually to K-Ras4B resistance to farnesyltransferase inhibitors, *J. Biol. Chem. 278*, 41718−41727.
21. Reuther, G. W., and Der, C. J. (2000) The Ras branch of small GTPases: Ras members don't fall far from the tree, *Curr. Opin. Cell Biol. 12*, 157−165.
22. Long, S. B., Casey, P. J., and Beese, L. S. (2000) The basis for K-Ras4B binding specificity to protein farnesyltransferase revealed by 2 angstrom resolution ternary complex structures, *Struct. Fold. Des. 8*, 209−222.
23. Taylor, J. S., Reid, T. S., Terry, K. L., Casey, P. J., and Beese, L. S. (2003) Structure of mammalian protein geranylgeranyltransferase type-I, *EMBO J. 22*, 5963−5974.
24. Rowell, C. A., Kowalczyk, J. J., Lewis, M. D., and Garcia, A. M. (1997) Direct demonstration of geranylgeranylation and farnesylation of Ki-Ras *in vivo*, *J. Biol. Chem. 272*, 14093−14097.
25. Whyte, D. B., Kirschmeier, P., Hockenberry, T. N., Nunez-Oliva, I., James, L., Catino, J. J., Bishop, W. R., and Pai, J. (1997) K- and N-Ras are geranylgeranylated in cells treated with farnesyl protein transferase inhibitors, *J. Biol. Chem. 272*, 14459−14464.
26. Adamson, P., Marshall, C. J., Hall, A., and Tilbrook, P. A. (1992) Post-translational modification of p21rho proteins, *J. Biol. Chem. 267*, 20033−20038.
27. Chen, Z., Sun, J. Z., Pradines, A., Favre, G., Adnane, J., and Sebti, S. M. (2000) Both farnesylated and geranylgeranylated RhoB inhibit malignant transformation and suppress human tumor growth in nude mice, *J. Biol. Chem. 275*, 17974−17978.
28. Du, W., Lebowitz, P. F., and Prendergast, G. C. (1999) Cell growth inhibition by farnesyltransferase inhibitors is mediated by gain of geranylgeranylated RhoB, *Mol. Cell. Biol. 19*, 1831−1840.
29. Riddles, P. W., Blakeley R. L., and Zerner, B. (1979) Ellman's reagent: 5,5′-dithiobis (2-nitrobenzoic acid)—a reexamination, *Anal. Biochem. 94*, 75−81.
30. Zimmerman, K. K., Scholten, J. D., Huang, C. C., Fierke, C. A., and Hupe, D. J. (1998) High-level expression of rat farnesyl: protein transferase in *Escherichia coli* as a translationally coupled heterodimer, *Protein Expression Purif. 14*, 395−402.
31. Bowers, K. E., and Fierke, C. A. (2004) Positively charged side chains in protein farnesyltransferase enhance catalysis by stabilizing the formation of the diphosphate leaving group, *Biochemistry 43*, 5256−5265.
32. Cassidy, P. B., Dolence, J. M., and Poulter, C. D. (1995) Continuous fluorescence assay for protein farnesyltransferase, *Methods Enzymol. 250*, 30−43.
33. Pompliano, D. L., Gomez, R. P., and Anthony, N. J. (1992) Intramolecular fluorescence enhancement: A continuous assay of Ras farnesyl:protein transferases, *J. Am. Chem. Soc. 114*, 7945−7946.
34. Chehade, K. A., Kiegiel K., Isaacs, R. J., Pickett, J. S., Bowers, K. E., Fierke, C. A., Andres, D. A., and Spielmann, H. P. (2002) Photoaffinity analogues of farnesyl pyrophosphate transferable by protein farnesyl transferase, *J. Am. Chem. Soc. 124*, 8206−8219.
35. Sagami, H., Korenaga, T., Ogura, K., Steiger, A., Pyun, H., and Coates, R. M. (1992) Studies on geranylgeranyl diphosphate synthase from rat liver: Specific inhibition by 3-azageranylgeranyl diphosphate, *Arch. Biochem. Biophys. 297*, 314−320.
36. Pais, J. E., Bowers, K. E, Stoddard, A. K., and Fierke, C. A. (2005) A continuous fluorescent assay for protein prenyltransferases measuring diphosphate release, *Anal. Biochem. 345*, 302−311.
37. Fersht, A. (1999) *Structure and Mechanism in Protein Science: A Guide to Enzyme Catalysis and Protein Folding*, W. H. Freeman and Company, New York.
38. Zhang, F. L., Kirschmeier, P., Carr, D., James, L., Bond, R. W., Wang, L., Patton, R., Windsor, W. T., Syto, R., Zhang, R. M., and Bishop, W. R. (1997) Characterization of Ha-Ras, N.-Ras, Ki-Ras4A, and Ki-Ras4B as *in vitro* substrates for farnesyl protein transferase and geranylgeranyl protein transferase type I, *J. Biol. Chem. 272*, 10232−10239.
39. Hightower, K. E., Casey, P. J., and Fierke, C. A. (2001) Farnesylation of nonpeptidic thiol compounds by protein farnesyltransferase, *Biochemistry 40*, 1002−1010.
40. Zhang, F. L., and Casey, P. J. (1996) Influence of metal ions on substrate binding and catalytic activity of mammalian protein geranylgeranyltransferase type-I, *Biochem. J. 320*, 925−932.
41. Grubbs, R. D. (2002) Intracellular magnesium and magnesium buffering, *BioMetals 15*, 251−259.
42. Saderholm, M. J., Hightower, K. E., and Fierke, C. A. (2000) Role of metals in the reaction catalyzed by protein farnesyltransferase, *Biochemistry 39*, 12398−12405.

43. Long, S. B., Casey, P. J., and Beese, L. S. (2002) Reaction path of protein farnesyltransferase at atomic resolution, *Nature 419*, 645−650.
44. Pickett, J. S., Bowers, K. E., Hartman, H. L., Fu, H., Embry, A. C., Casey, P. J., and Fierke, C. A. (2003) Kinetic studies of protein farnesyltransferase mutants establish active substrate conformation, *Biochemistry 42*, 9741−9748.
45. Mazières, J., Tillement, V., Allal, C., Clanet, C., Bobin, L., Chen, Z., Sebti, S. M., Favre, G., and Pradines, A. (2005) Geranylgeranylated, but not farnesylated, RhoB suppresses Ras transformation of NIH-3T3 cells, *Exp. Cell Res. 304*, 354−364.

BI050951V